1

Introduction

1.1 Introduction

High data-rate wireless communications, nearing 1 Gb/s transmission rates, are of interest in emerging wireless local area networks (WLANs) and in home audio/video network applications, such as high-speed high-definition television (HDTV) audio/video streams [189]. Currently, WLANs offer peak rates up to 54 Mb/s, and a target of 600 Mb/s is promised to be realized in the near future, for example, in IEEE 802.11n WLANs [72]. The IEEE 802.15.3c wireless personal area networks (WPANs) will allow very high data rates of over 2 Gb/s for applications such as high-speed internet access, streaming content download (for example, video on demand, HDTV, home theatre), real-time streaming, and wireless data bus for cable replacement. Optional data rates in excess of 3 Gb/s will be provided. However, to achieve, say, more than 50 Mb/s data rates, some technologies such as multiple transmit and multiple receive antennas (MIMO) and orthogonal frequency-division multiplexing (OFDM) should be adopted, as recommended in IEEE 802.11n. To reach the target of 1 Gb/s, more advanced techniques should be used. Ultra wideband (UWB) technology combined with MIMO might provide a solution.

As is well known, a UWB system [22, 165, 243, 264] can make use of the huge frequency band from 3.1 to 10.6 GHz in the USA [63] and Asia [49] and at least 6.0 to 8.5 GHz in Europe [105][1]. This provides great potential for increasing data transmission rates according to the Shannon theorem. However, owing to the regulations imposed by the Federal Communications Commission (FCC) in the USA [63] and the European Commission (EC) document in Europe [105], the permitted power spectral density of a UWB signal is rather limited. This again limits data transmission rates. Incorporating the MIMO technique into UWB provides a viable solution for the bottleneck problem of power limit. For example, if space–time coding (STC) is used, the power for a specific transmitted symbol will be strengthened, while the overall transmitted power is still the same as that of a single-transmit-antenna system, thus satisfying the FCC regulation (see Chapter 4). If a beamforming technique is employed, the power of the signal in a specific direction is increased and may violate the power spectral mask in this direction,

[1] In Europe, the frequency band from 1.6 to 10.6 GHz can be used, but a stricter spectral mask is specified than that in the USA. For the details, see [105].

Ultra Wideband Systems with MIMO Thomas Kaiser and Feng Zheng

while the power in all other directions is still the same as the case without using the beamformer (see Chapter 5 about the side lobe discussion of UWB beamformers).

One may argue about why UWB should be combined with the MIMO technology, since UWB itself offers rich diversity owing to its abundant multipaths. A simple answer to this question is that it is due to the general greed of ones' pursuing higher data rates and higher quality of communications; but this is not the whole picture for the problem. According to Edholm's law of data rate [44], it can be predicted that indoor data rates of several gigabits per second will become a reality in a couple of years. Therefore, although UWB offers enormous bandwidth and, hence, rich diversity in the time domain, even more bandwidth will be required in the near future. Hence, if it can be shown that the channel capacity of UWB systems is proportional to the number of transmit/receive antennas (this is indeed the case; see Chapter 3), then data rates can be significantly increased further by combining UWB and MIMO. This reason is the same as the one that triggered the research era on MIMO about two decades ago [268]. Even if lower data rates are in focus, the trade-off between bandwidth and the number of antennas could facilitate the antenna and amplifier design, which is still a challenge for UWB systems. For example, the bandwidth requirement could be reduced by almost half if two antennas, instead of one antenna, on both transmitter and receiver sides are deployed.[2]

In this book, we investigate the benefits of combining UWB and MIMO. We highlight five aspects of this promising research field: channel capacity, STC, beamforming, UWB-MIMO relay and time-reversal (TR) transmission. The channel capacity describes a limit of the benefits in some sense for a UWB system employing multiple antennas, while STC provides a realization tool towards reaching the limit. UWB beamforming is of great importance for indoor localization, which has become a hot topic in UWB applications. The TR modulation provides a nontraditional, yet promising, way for secure and/or multi-user wireless communications. UWB-MIMO relay provides an important tool for UWB communications in non-line-of-sight (NLOS) environments where the direct link between communication partners is blocked or the distance is too great.

1.2 UWB Basics

A UWB transmission system, by definition [63, 210], is a radio system whose 10 dB bandwidth $(f_H - f_L)$ is at least 500 MHz and whose fractional bandwidth $(f_H - f_L)/[(f_H + f_L)/2]$ is at least 20 %. A UWB radio system can coexist with other kinds of narrow- and wide-band radio systems. Hence, its power spectrum density is strictly limited by relevant regulatory authorities. In the USA, a UWB device can use the frequency band from 3.1 to 10.6 GHz under the spectral mask specified in [63], as illustrated in Figure 1.1 for the indoor applications of the UWB. Notice that different permitted equivalent isotropically radiated power (EIRP) emission levels are applied to different UWB application categories, but in most applications the magic figure −41.3 dBm/MHz across the 3.1 to

[2] Consider the case where we want to achieve a fixed data rate, say R_0, by using a single transmit and single receive antenna (SISO) UWB system (denoted as S_1) and a 2×2 MIMO UWB system (denoted as S_2). Except for bandwidth, all other system parameters and configurations (for example, modulations and coding–decoding techniques) are the same for S_1 and S_2. Suppose the bandwidth required by system S_1 to achieve R_0 is B_1. Since the channel capacity of S_2 is doubled compared with that of S_1 if they have the same bandwidth, system S_2 will require only a bandwidth of $B_1/2$ to achieve the same data rate R_0.

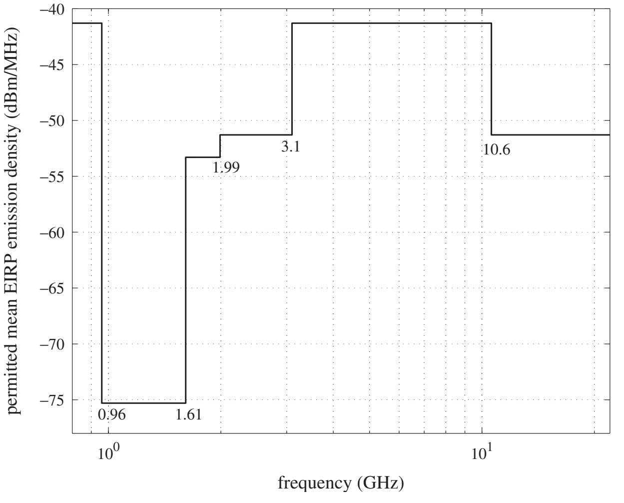

Figure 1.1 FCC spectral mask for UWB indoor applications.

10.6 GHz frequency band applies. In Europe, a further wide frequency band from 1.6 to 10.6 GHz can be used, but a more strict spectral mask is specified than that in the USA; see Figure 1.2 for an illustration and [105] for the details. In Asia, some proposals for the spectral masks have been proposed, but final concurrence has not yet been reached [49].

There are two approaches to implementing this kind of radio system. The first is the impulse radio (IR)-based approach, where a pulse train, in which each pulse is very short in the time domain (typically on the order of several tens of picoseconds), is used to carry out information data. This pulse train will be directly transmitted through the

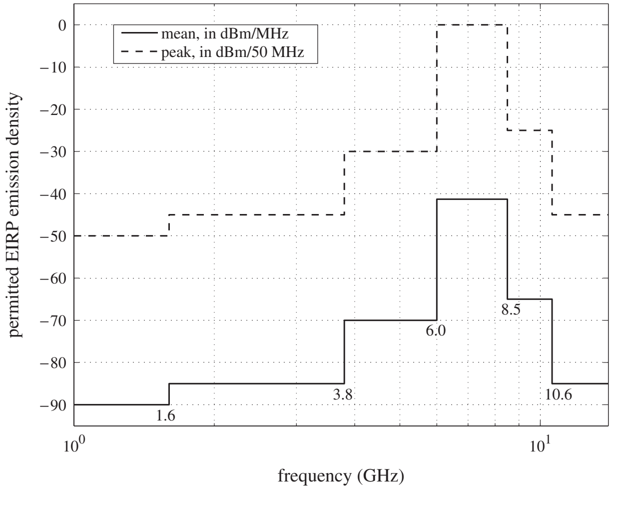

Figure 1.2 EU spectral mask for UWB indoor applications.

antenna without any carriers. The second is the multiband (MB)-based approach, where the information data is multiplexed into sub-frequency bands in the entire band from 3.1 to 10.6 GHz or a part of it, with each sub-band having 528 MHz bandwidth. In each sub-band, the information data is transmitted by using traditional multi-carrier orthogonal frequency-division multiplexing (OFDM) technology.

The main advantage of the IR-based UWB systems is the simplicity in the transceiver structure. No up- and down-mixers are needed in this kind of system. This advantage is one of the most important reasons which boosted our interest in UWB systems at the very beginning of UWB-related studies. The drawback of the IR-based UWB systems is the large number of multipaths, typically on the order from several tens to a hundred more [265, 267] for a normal office environment. This causes a big challenge for the synchronizer design with reasonably quick acquisition time and the rake receiver implementation with sufficient fingers to capture enough energy.

The main advantage of the MB-based UWB systems is that the key OFDM technique is already mature for deployment in the market, and its several nice properties, such as high spectral efficiency, inherent resilience to radio-frequency (RF) interference, robustness to multipaths, and the ability to efficiently capture multipath energy, have been proven in other commercial technologies, for example, in IEEE 802.11a/g [1, 2]. The drawback of the MB-based UWB systems is the complexity involved in implementing up- and down-mixers and OFDM. The latter requires fast Fourier transform (FFT) and inverse FFT (IFFT) algorithms at the receiver and transmitter sides respectively [192]. This is not preferable in typical UWB applications.

Currently, it is controversial about which technology will dominate the future market, due to the various pros and cons of these two technologies. However, the IR-based UWB technology is finding its niche in some applications such as indoor wireless localization. Therefore, we will focus our main attention on the IR-based UWB systems in this book.

The popularly used waveforms for the monopulse in the IR-based UWB systems are the first and second derivatives of the Gaussian monopulse [264, 267], which are defined respectively by

$$w_1(t) = \varsigma_1 t \exp\left[-2\pi\left(\frac{t}{\tau_\mathrm{p}}\right)^2\right],$$

$$w_2(t) = \varsigma_2 \left[1 - 4\pi\left(\frac{t}{\tau_\mathrm{p}}\right)^2\right] \exp\left[-2\pi\left(\frac{t}{\tau_\mathrm{p}}\right)^2\right],$$

where τ_p is a parameter used to adjust the pulse width and ς_1 and ς_2 are two constants to normalize the peak amplitudes or powers of the pulses $w_1(t)$ and $w_2(t)$ respectively. Generally, the original Gaussian monopulse

$$w_0(t) = \varsigma_0 \exp\left[-2\pi\left(\frac{t}{\tau_\mathrm{p}}\right)^2\right]$$

is not adopted since its power spectrum contains a DC component. The monopulses w_1 and w_2 are illustrated in Figure 1.3.

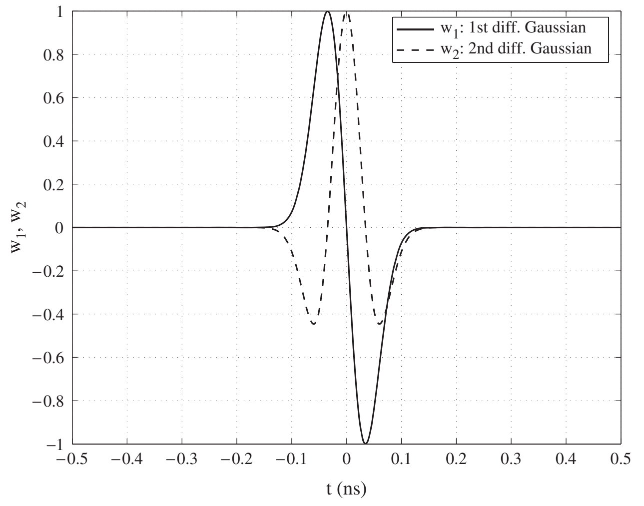

Figure 1.3 The basic monopulses for IR-based UWB systems ($\tau_p = 0.1225\,\text{ns}$).

The information data can be embedded in either the amplitude or the position of the UWB impulse train to transmit, producing pulse-amplitude modulation (PAM) and pulse-position modulation (PPM) respectively. For multi-user access to the UWB channel, there are basically two kinds of accessing techniques: time hopping (TH) spread spectrum (SS) and direct sequence (DS) SS accessing. Since the transmit power is rather low, one information bit in the IR-based UWB system is generally spread over multiple monocycles to achieve a processing gain in reception.

For TH-SS accessing, the data modulation can be generally expressed as [209, 266, 274]

$$s_k(t) = \sum_{j=-\infty}^{\infty} a_k(\lfloor j/N_f \rfloor) w\left(t - jT_f - c_k(j)T_c - \delta d_k(\lfloor j/N_f \rfloor)\right), \tag{1.1}$$

where $\lfloor x \rfloor$ denotes the integer floor of x, s_k is the transmitted signal for the kth user, $w(t)$ is the monopulse of duration T_w, N_f is the number of frames for one data symbol, T_f is the frame duration, T_c is the chip duration, δ is the modulation index, $\{c_k(j)\}$ is the TH coding sequence, which takes values in $[0, N_c - 1]$ and is assumed to be periodic with period N_f, and a_k and d_k are the transmitted data symbols.

It is assumed that $T_f = N_c T_c$ with N_c being the number of chips in one frame duration, $T_w \ll T_c$, and $\delta \ll T_c$.

If $a_k = 1$, then Equation (1.1) reduces to TH-SS-PPM. If $d_k = 0$, then Equation (1.1) reduces to TH-SS-PAM. Clearly, the power spectral density (PSD) of the transmitted signal depends on the spectra of both the monopulse and transmitted data sequence. Therefore, it is the combination of the monopulse and transmitted data sequence that shapes the PSD of the transmitted signal and, hence, satisfies the required spectral mask. A complete analysis of the PSD of the transmitted signal is provided in [262].

For DS-SS accessing, the data modulation is expressed as [274, 292]

$$s_k(t) = \sum_{j=-\infty}^{\infty} a_k(\lfloor j/N_{\mathrm{f}} \rfloor) c_k(j) w\left(t - jT_{\mathrm{f}} - \delta d_k(\lfloor j/N_{\mathrm{f}} \rfloor)\right). \tag{1.2}$$

Early research on UWB for wireless communications focused on TH-SS PPM due to its implementation advantage of not requiring to change, or inverse for binary modulation, the pulse amplitude [292]. Besides, the PSD of a TH-SS PPM signal does not have strong spectral lines, since the TH information sequence smoothes the PSD of the transmitted signal, which is a big advantage of the TH-SS PPM scheme because the strong spectral lines will introduce noticeable interference to other radio systems in the same frequency band [274, 292].

1.3 MIMO Principle

To see the benefit of MIMO, let us investigate the signal-to-noise power ratio (SNR) or channel capacity gain of the MIMO compared with that of SISO for narrowband wireless communication systems with frequency-flat channels. Since many kinds of system performance (such as channel capacity, data rates, bit error rates, etc.) are determined by the SNR, it is justifiable by investigating the SNR gain of the MIMO systems. To make the comparison fair, we keep the constraint that the transmit power of the MIMO is the same as that of the SISO. Let N_{T} and N_{R} be the numbers of transmit and receive antennas respectively.

First consider the single transmit antenna and multiple receive antennas (SIMO) case. The input–output relationship can be expressed as

$$Y_i(t) = h_i X(t) + N_i(t), \tag{1.3}$$

where $X(t)$ and $Y_i(t)$, $i = 1, \ldots, N_{\mathrm{R}}$, are the transmit signal and receive signals respectively, h_i, $i = 1, \ldots, N_{\mathrm{R}}$, are the channel fading from the transmitter to each receiver, and $N_i(t)$, $i = 1, \ldots, N_{\mathrm{R}}$, are the receiver noises with zero mean and variance σ_N^2. For the SISO case, the input–output relationship is expressed as

$$Y(t) = hX(t) + N(t),$$

where the symbols have the same meaning as those in Equation (1.3) and the noise $N(t)$ is also of zero mean and variance σ_N^2. Suppose that all h and h_i, $i = 1, \ldots, N_{\mathrm{R}}$, are complex Gaussian with zero mean and variances σ_h^2 and $\sigma_{h_i}^2$ respectively. Suppose that $X(t)$, h_i, h, $N_i(t)$ and $N(t)$ are mutually independent.

If the receiver does not have the channel state information (CSI), we can combine the received signals with an equal gain, i.e.:

$$Y_{\mathrm{SIMO}}(t) = \sum_{i=1}^{N_{\mathrm{R}}} Y_i(t) = \sum_{i=1}^{N_{\mathrm{R}}} h_i X(t) + \sum_{i=1}^{N_{\mathrm{R}}} N_i(t).$$

Then the SNR of the combined signal is

$$\begin{aligned}\mathrm{SNR}_{\mathrm{SIMO}} &= \frac{\mathbb{E}\left\{\left[\sum_{i=1}^{N_\mathrm{R}} h_i X(t)\right]\left[\sum_{i=1}^{N_\mathrm{R}} h_i X(t)\right]^*\right\}}{\mathbb{E}\left\{\left[\sum_{i=1}^{N_\mathrm{R}} N_i(t)\right]\left[\sum_{i=1}^{N_\mathrm{R}} N_i(t)\right]^*\right\}} = \frac{\sum_{i=1}^{N_\mathrm{R}} \sigma_{h_i}^2}{N_\mathrm{R}} \frac{\mathbb{E}[|X(t)|^2]}{\sigma_N^2} \\ &= \frac{\sum_{i=1}^{N_\mathrm{R}} \sigma_{h_i}^2}{N_\mathrm{R}} \mathrm{SNR}_\mathrm{T}, \end{aligned} \tag{1.4}$$

where SNR_T denotes the SNR at the transmitter side. From Equation (1.4) we can see that there is no gain in the SNR if the receiver does not know the CSI.

On the other hand, if the receiver knows the CSI, then the receiver can combine the received signals using the maximum ratio combiner (MRC) as follows:

$$Y_{\mathrm{SIMO}}(t) = \sum_{i=1}^{N_\mathrm{R}} h_i^* Y_i(t) = \sum_{i=1}^{N_\mathrm{R}} |h_i|^2 X(t) + \sum_{i=1}^{N_\mathrm{R}} h_i^* N_i(t).$$

Then the SNR gained is

$$\begin{aligned}&\mathrm{SNR}_{\mathrm{SIMO}} \\ &= \frac{\mathbb{E}\left\{\left[\sum_{i=1}^{N_\mathrm{R}} |h_i|^2 X(t)\right]\left[\sum_{i=1}^{N_\mathrm{R}} |h_i|^2 X(t)\right]^*\right\}}{\mathbb{E}\left\{\left[\sum_{i=1}^{N_\mathrm{R}} h_i^* N_i(t)\right]\left[\sum_{i=1}^{N_\mathrm{R}} h_i^* N_i(t)\right]^*\right\}} \\ &= \frac{\mathbb{E}\left[\sum_{i=1}^{N_\mathrm{R}} |h_i|^4\right]\mathbb{E}[|X(t)|^2] + \mathbb{E}\left\{\left[\sum_{i_1=1}^{N_\mathrm{R}} |h_{i_1}|^2\right]\left[\sum_{i_2=1, i_2\neq i_1}^{N_\mathrm{R}} |h_{i_2}|^2\right]\right\}\mathbb{E}[|X(t)|^2]}{\mathbb{E}\left[\sum_{i_1=1}^{N_\mathrm{R}} |h_{i_1}|^2\right]\sigma_N^2} \\ &= \frac{2\sum_{i=1}^{N_\mathrm{R}} \sigma_{h_i}^4 + \sum_{i_1=1}^{N_\mathrm{R}} \sum_{i_2=1, i_2\neq i_1}^{N_\mathrm{R}} \sigma_{h_{i_1}}^2 \sigma_{h_{i_2}}^2}{\sum_{i=1}^{N_\mathrm{R}} \sigma_{h_i}^2} \frac{\mathbb{E}[|X(t)|^2]}{\sigma_N^2} \\ &= \left(\frac{\sum_{i_1=1}^{N_\mathrm{R}} \sigma_{h_i}^4}{\sum_{i_1=1}^{N_\mathrm{R}} \sigma_{h_i}^2} + \sum_{i_1=1}^{N_\mathrm{R}} \sigma_{h_i}^2\right) \mathrm{SNR}_\mathrm{T}. \end{aligned} \tag{1.5}$$

In the third equality we have used the property $\mathbb{E}[|h_i|^4] = 2\sigma_{h_i}^4$ of complex Gaussian random variables [101, p. 91], [122]. From Equation (1.5) we can see that the SNR is increased exactly N_R-fold (i.e., the SNR of the SIMO is $(N_\mathrm{R}+1)$-times that of the SISO) by using the MRC if the CSI is available at the receiver and all the links in the SIMO have the same fading power as the link in the SISO.

Next, consider the multiple transmit antennas and single receive antenna (MISO) case. The input–output relationship can be expressed as

$$Y(t) = \sum_{i=1}^{N_\mathrm{T}} h_i X_i(t) + N(t), \tag{1.6}$$

where $Y(t)$ is the receive signal, $X_i(t)$, $i = 1, \ldots, N_{\mathrm{T}}$, are the transmit signals and h_i, $i = 1, \ldots, N_{\mathrm{T}}$, is the channel fading from each transmitter to the receiver. For the statistical properties of the model (1.6), we make similar assumptions as those for model (1.3) except that $\mathbb{E}[|X_i(t)|^2] = \mathbb{E}[|X(t)|^2]/N_{\mathrm{T}}$, where $\mathbb{E}[|X(t)|^2]$ is the power of the transmit signal for the SISO case.

If the transmitter does not have the CSI, then the SNR achieved at the receiver will be

$$\begin{aligned}\mathrm{SNR_{MISO}} &= \frac{\mathbb{E}\left\{\left[\sum_{i=1}^{N_{\mathrm{T}}} h_i X_i(t)\right]\left[\sum_{i=1}^{N_{\mathrm{T}}} h_i X_i(t)\right]^*\right\}}{\mathbb{E}\{|N(t)|^2\}} = \frac{\sum_{i=1}^{N_{\mathrm{T}}} \sigma_{h_i}^2}{N_{\mathrm{T}}} \frac{\mathbb{E}[|X(t)|^2]}{\sigma_N^2} \\ &= \frac{\sum_{i=1}^{N_{\mathrm{T}}} \sigma_{h_i}^2}{N_{\mathrm{T}}} \mathrm{SNR_T}.\end{aligned}$$

It can be seen that there is no gain in the received SNR.

On the other hand, if the transmitter knows the CSI, then it can preprocess the transmitted signal for each transmit antenna so that some gain is achieved in the received SNR. Suppose the transmitted signal for each transmit antenna is weighted by its channel fading:

$$X_i(t) \longrightarrow \frac{h_i^*}{\sqrt{\sum_{i=1}^{N_{\mathrm{T}}} \sigma_{h_i}^2}} X_i(t).$$

Note that $\mathbb{E}[|X_i(t)|^2] = \mathbb{E}[|X(t)|^2]$ in this situation. Then the overall transmitted power will be the same as the SISO case, and the received signal is

$$Y(t) = \frac{1}{\sqrt{\sum_{i=1}^{N_T} \sigma_{h_i}^2}} \sum_{i=1}^{N_{\mathrm{T}}} h_i h_i^* X_i(t) + N(t).$$

Thus the received SNR is

$$\begin{aligned}&\mathrm{SNR_{MISO}} \\ &\quad = \frac{\left(1/\sum_{i=1}^{N_{\mathrm{T}}} \sigma_{h_i}^2\right) \mathbb{E}\left\{\left[\sum_{i=1}^{N_{\mathrm{T}}} |h_i|^2 X_i(t)\right]\left[\sum_{i=1}^{N_{\mathrm{T}}} |h_i|^2 X_i(t)\right]^*\right\}}{\mathbb{E}\{|N(t)|^2\}} \\ &\quad = \frac{\mathbb{E}\left[\sum_{i=1}^{N_{\mathrm{T}}} |h_i|^4 |X_i(t)|^2\right] + \mathbb{E}\left\{\left[\sum_{i_1=1}^{N_{\mathrm{T}}} |h_{i_1}|^2 X_{i_1}(t)\right]\left[\sum_{i_2=1, i_2 \neq i_1}^{N_{\mathrm{T}}} |h_{i_2}|^2 X_{i_2}(t)\right]^*\right\}}{\sigma_N^2 \sum_{i=1}^{N_{\mathrm{T}}} \sigma_{h_i}^2}.\end{aligned}$$

Let us divide the problem into two cases. The first case is that $X_{i_1}(t)$ and $X_{i_2}(t)$ are different streams of symbols for $i_1 \neq i_2$ and are mutually independent with zero mean. This corresponds to the case of multiplexing. Then

$$\mathrm{SNR_{MISO}} = \frac{2\sum_{i=1}^{N_{\mathrm{T}}} \sigma_{h_i}^4 \mathbb{E}[|X_i(t)|^2]}{\sigma_N^2 \sum_{i=1}^{N_{\mathrm{T}}} \sigma_{h_i}^2} = \frac{2\sum_{i=1}^{N_{\mathrm{T}}} \sigma_{h_i}^4}{\sum_{i=1}^{N_{\mathrm{T}}} \sigma_{h_i}^2} \frac{\mathbb{E}[|X(t)|^2]}{\sigma_N^2} = \frac{2\sum_{i=1}^{N_{\mathrm{T}}} \sigma_{h_i}^4}{\sum_{i=1}^{N_{\mathrm{T}}} \sigma_{h_i}^2} \mathrm{SNR_T}.$$

If all the links have the same fading power as the SISO link, then we can see that the received SNR is doubled compared with the SISO case. Notice that the symbol rate of the MISO in this case is N_{T}-times that of the SISO.

The second case is that $X_{i_1}(t) = X_{i_2}(t)$ for all i_1 and i_2 and all are of zero mean. This corresponds to the case of diversity combining. In this case, we have

$$\begin{aligned}
&\mathrm{SNR}_{\mathrm{MISO}} \\
&= \frac{\mathbb{E}\left[\sum_{i=1}^{N_\mathrm{T}} |h_i|^4 |X_i(t)|^2\right] + \mathbb{E}\left\{\left[\sum_{i_1=1}^{N_\mathrm{T}} |h_{i_1}|^2 X_{i_1}(t)\right]\left[\sum_{i_2=1, i_2\neq i_1}^{N_\mathrm{T}} |h_{i_2}|^2 X_{i_2}(t)\right]^*\right\}}{\sigma_N^2 \sum_{i=1}^{N_\mathrm{T}} \sigma_{h_i}^2} \\
&= \frac{\mathbb{E}\left[\sum_{i=1}^{N_\mathrm{T}} |h_i|^4\right] \mathbb{E}[|X_i(t)|^2] + \mathbb{E}\left\{\left[\sum_{i_1=1}^{N_\mathrm{T}} |h_{i_1}|^2\right]\left[\sum_{i_2=1, i_2\neq i_1}^{N_\mathrm{T}} |h_{i_2}|^2\right]\right\} \mathbb{E}[|X_i(t)|^2]}{\sigma_N^2 \sum_{i=1}^{N_\mathrm{T}} \sigma_{h_i}^2} \\
&= \frac{2\sum_{i=1}^{N_\mathrm{T}} \sigma_{h_i}^4 + \sum_{i_1=1}^{N_\mathrm{T}} \sum_{i_2=1, i_2\neq i_1}^{N_\mathrm{T}} \sigma_{h_{i_1}}^2 \sigma_{h_{i_2}}^2}{\sum_{i=1}^{N_\mathrm{T}} \sigma_{h_i}^2} \frac{\mathbb{E}[|X(t)|^2]}{\sigma_N^2} \\
&= \left(\frac{\sum_{i_1=1}^{N_\mathrm{T}} \sigma_{h_i}^4}{\sum_{i_1=1}^{N_\mathrm{T}} \sigma_{h_i}^2} + \sum_{i_1=1}^{N_\mathrm{T}} \sigma_{h_i}^2\right) \mathrm{SNR}_\mathrm{T}.
\end{aligned}$$

This leads to the same result as the SIMO case, i.e., the SNR is increased exactly N_T-fold by using the preprocessing technique if the CSI is available at the transmitter and all the links in the MISO have the same fading power as the link in the SISO.

Now consider the MIMO case. The input–output relationship can be expressed as

$$\mathbf{Y}(t) = \mathbf{H}\mathbf{X}(t) + \mathbf{N}(t),$$

where $\mathbf{X}(t)$, $\mathbf{Y}(t)$, $\mathbf{H}$ and $\mathbf{N}(t)$ are the N_T-dimensional transmit signal, the N_R-dimensional receive signal, the $(N_\mathrm{R} \times N_\mathrm{T})$-dimensional channel matrix and the N_R-dimensional receiver noise respectively. Let us express $\mathbf{H}$ in the singular value decomposition form [107, p. 414]:

$$\mathbf{H} = \mathbf{U}\boldsymbol{\Sigma}\mathbf{V}^*,$$

where $\mathbf{U}$ and $\mathbf{V}$ are unitary matrices of $N_\mathrm{R} \times N_\mathrm{R}$ and $N_\mathrm{T} \times N_\mathrm{T}$ dimensions respectively, $\boldsymbol{\Sigma} = [\sigma_{ij}]$ is an $(N_\mathrm{R} \times N_\mathrm{T})$-dimensional diagonal matrix in the sense of $\sigma_{ij} = 0$ for all $i \neq j$. The diagonal entries σ_{ii} are of the property $\sigma_{11} \geq \sigma_{22} \geq \cdots \geq \sigma_{N_\mathrm{TR}N_\mathrm{TR}} \geq 0$, where $N_\mathrm{TR} = \min\{N_\mathrm{T}, N_\mathrm{R}\}$. If $\mathbf{H}$ is of full rank (this holds true generally for a random matrix), then we have $\sigma_{N_\mathrm{TR}N_\mathrm{TR}} > 0$. Suppose that the CSI $\mathbf{H}$ is available at both transmitter and receiver. Let us preprocess and post-process the transmit signal and receive signal respectively in the following way:

$$\bar{\mathbf{X}}(t) = \mathbf{V}^*\mathbf{X}(t), \quad \bar{\mathbf{Y}}(t) = \mathbf{U}^*\mathbf{Y}(t),$$

where $\bar{\mathbf{X}}(t)$ and $\bar{\mathbf{Y}}(t)$ are new transmit and receive signals respectively. Then we have

$$\bar{\mathbf{Y}}(t) = \boldsymbol{\Sigma}\bar{\mathbf{X}}(t) + \mathbf{U}^*\mathbf{N}(t). \tag{1.7}$$

From Equation (1.7) we can see that the new MIMO channel is equivalent to N_TR independent channels, each having the same bandwidth. If spatial multiplexing is used, then it can be easily seen that the data transmission rate can be increased N_TR-fold on average compared with the SISO channel. From the viewpoint of channel capacity, the ergodic channel capacity [24, 90] of the MIMO channel can also be increased N_{TR}-fold compared with the SISO channel, since this capacity is determined by the determinant of the matrix $\mathbf{I} + \mathbf{H}\mathbf{H}^*$ [244].

From the above discussion, one can see that the MIMO technology can yield a considerable gain in system performance compared with the SISO system.

1.4 State-of-the-Art UWB-MIMO

UWB technology has been widely used in radar and information sensing for more than 30 years. The study of UWB for communications started during the late 1990s. A dramatic change in the study happened in 2002, when the US FCC issued the regulation on the spectral mask of UWB radios. Under the regulation, the extremely wide radio spectrum from 3.1 to 10.6 GHz can be freely used without a licence application if the transmission satisfies the spectral mask condition. This event triggered a great interest in the community of wireless communications from both academia and industry. Since then, almost all concepts, ideas and techniques in narrow- or wide-band wireless communications have been immigrated into UWB communications. However, UWB-MIMO is still in its research infancy. The reason might be twofold. First, MIMO itself is a quite new technology. Its implementation in practical communication equipment is a recent matter. Second, a UWB channel itself possesses rich diversity due to its abundant multipaths. This raises some doubt about whether it is necessary to combine MIMO with UWB. It is our belief that UWB-MIMO will become a powerful candidate for extremely high data-rate communications in the near future. The recent surge of research reports on UWB-MIMO also verifies this belief.

Compared with the volumes of literature in narrowband MIMO research, there are only a few studies of UWB-MIMO. Basically, these studies can be categorized into four fields: UWB-MIMO channel measurement and modelling, channel capacity, STC and beamforming.

With regard to channel measurements and characterizations, several reports have been published; for example, see [123, 152, 156]. The full characterization of the spatial correlation of UWB channels is provided in [152], where it is found that in the range of 2.5 times the coherence distance (about 4 cm) the antenna correlation follows a pattern of the first kind zeroth-order Bessel function with distance, while an almost constant correlation coefficient (smaller than 0.4) is observed when the antenna distance is greater than 2.5 times the coherence distance. It is particularly interesting that, as shown in [65, 114, 152, 155, 156], the antenna angular orientation and the signal polarization can be used to decrease the correlation of the spatial channels or to improve the system performance. Another approach describing the correlation property is from the deterministic viewpoint [247]. It is defined as the average value of all the cross-correlation functions of different spatial channels normalized by the autocorrelation functions of corresponding spatial channels. A possible unfavourable electromagnetic coupling between UWB antenna elements has been proven to be small, even for marginal antenna separations [216].

Regarding the channel capacity of UWB-MIMO systems, the research results can be found in [159, 197, 284, 285, 287]. In [284, 285], it is shown that for N_T transmit and

N_R receive antennas (for simplicity, it is assumed that $N_T = N_R$ there) the UWB-MIMO ergodic channel capacity increases linearly with N_R. However, for the MISO case, it is not always beneficial to employ more transmit antennas. It is shown in [284, 285, 287] that the outage probability decreases with the number of transmit antennas when the communication rate is lower than the critical transmission rate, but it increases when the rate is higher than another value. This critical transmission rate is determined by the fading power and the SNR of the system at the transmitter side. We can roughly say that it is not beneficial to use multiple transmit antennas if the required transmission rate (normalized by the system bandwidth) is higher than the critical transmission rate or equivalently when the available power at the transmitter side is too low. In [159], a fixed region of scattering environments for UWB-MIMO systems is considered. Thus, the number of spatial degrees of freedom of the scattered field, denoted η, is limited. It is shown in [159] that the system capacity is fundamentally limited by the three numbers N_T, N_R and η. This is not strange, since η will place a limit on the rank of the UWB-MIMO channel matrix; hence, it will affect the number of the independently separate channels. In [197], it is shown that if several different antennas (a loop antenna and two orthogonal bow-tie antennas there) are placed in the same place instead of separately in different places with sufficient distance as in the traditional spatial antenna array, the spectral efficiency of such a system approaches that of the traditional array system. This is due to the fact that the rank of the channel matrix involved is well maintained to be equal for both kinds of systems.

Since a UWB system is often required to work in a low power regime by the relevant regulation bodies, it is important to investigate the system capacity at low power or in a low SNR regime. For wideband systems, it is shown in [80, 171] that very large bandwidths yield poor performance for systems that spread the available power uniformly over time and frequency. In [245] it is shown that the input signals needed to achieve a capacity must be peaky in time or frequency for a wideband fading channel composed of a number of time-varying paths. We can witness this phenomenon for UWB-MIMO systems, as illustrated in [287]. In [287], the uniform power spectrum allocation (UPSA) and optimal power spectrum allocation (OPSA) policies are investigated for transmitted UWB signals, where, for the OPSA, a water-filling algorithm is applied to adjust the power distribution across both the frequency domain and the antenna domain according to the status of the channel multipath fading, and for the UPSA the transmitted power is uniformly distributed across both domains. It is demonstrated that the efficiency of the UPSA relative to the OPSA is low when the SNR is lower than -20 dB. However, when the SNR is higher than 10 dB, the UPSA policy almost produces the same channel capacity as the OPSA policy. Therefore, an optimal power distribution algorithm, such as the water-filling approach, should be considered if the SNR is rather low, while the water-filling algorithm is just to make the transmitted signals 'peaky' in both the frequency and the antenna domains. When the CSI is unknown at the receiver, the system performance is characterized in [203] for MIMO wideband systems.

For the STC, the first result was reported in [273] for IR UWB systems, where it is shown that the receive diversity order is equal to the product of the number of receive antennas and the number of rake fingers. Note that a larger number of antennas promises only a limited diversity gain because of the distinct UWB multipath diversity [260]. In [247], a spatial-multiplexing coherent scheme for a 2×2 UWB-MIMO system is experimentally investigated. In [251], the performance of a space–time trellis code for a 2×2 UWB-MIMO system is evaluated. For general IR-based UWB systems, the STC method was provided in [6, 7, 8, 225]. For OFDM-based UWB systems, [227] presented an STC method which was essentially similar to the STC for wideband OFDM. The report [258] showed an approach to increasing the spatial diversity via antenna selection across data frames. In [39], a space–time selective-rake receiver is proposed considering the presence of narrowband interference and multiple access interference. In [73], a time-interleaving multi-transmit-antenna UWB system is proposed, where monocycle pulses per information symbol are transmitted discontinuously through the time interleaver to get more temporal diversity. Spatial diversity and temporal diversity are compared therein. In [146], a zero-forcing scheme is proposed to remove the interference among the multiple data streams in UWB-MIMO systems. A space–time trellis coding scheme is proposed in [182]. In [238, 240, 260], the multiple access performance of UWB-MIMO systems is investigated. Spatial multiplexing is proposed in [129], where the VBLAST (vertical Bell Laboratory layered space–time) algorithm was applied to UWB systems and a significant multiplexing gain could be proven.

For UWB-MIMO STC, it is found [118] that a fundamental compromise exists among the available SNR, coding interval and the number of transmit antennas. The basic conclusion is that only when the available SNR is sufficiently high (supposing that the total power over all the transmit antennas and the coding interval is fixed), can the coding gain be obtained by deploying the transmit power into more transmit antennas and using a longer coding interval. In other words, if the available SNR is too low, then it is better to use less transmit antennas and shorter space–time codes. Therefore, we can see another kind of 'peaky' phenomenon again. It is highly expected to give some quantitative characterization for how high the SNR should be so that the STC can indeed provide rewarding gains. However, this is not available for general UWB-MIMO systems.

Regarding UWB beamforming, systematic studies of the problem were presented in [109, 110, 204], with several fundamental differences being found. In [115], a digital UWB beamforming scheme was proposed. The effect of multipaths on the beamformer output was illustrated in [174], which was simulated by using the ray-tracing technique. In [67, 68, 116], the UWB beamformer was used to find the location of the source. In [154], an adaptive beamformer for MB UWB wireless systems was proposed where it was shown that the signal bandwidth had little impact on the beamwidth or direction; hence, the beam focusing capability will not be sensitive to the signal bandwidth. In [231], the measured transient response of a uniform linear UWB array shows a peaked output without side lobes. In [88], an interesting algorithm for calculating the weighting coefficients of wideband beamformers was developed.

UWB Beamformers have some peculiar properties that are quite different from the narrowband beamformers. For example, the use of unequal weighting filters for the individual antenna branch increases the side-lobe level in UWB beamformers; thus, optimal beamformers, as shown in [204], are those in which the weighting filters for all the antenna branches are identical. A basic difficulty in the UWB beamformer is how to deal with multipaths of the inherited UWB signal propagations. In narrowband array processing technology, this problem can be ignored, but we cannot ignore it in the UWB array since the multipath is one of the most pronounced characteristics of UWB channels. In this research subfield, ranging [116, 117] and sensing are promising applications of multi-antenna UWB technology. Ultra-short pulses allow spatial resolution even down to subdecimetre range. By means of multi-antenna techniques, additional spatial parameters can be generally extracted (for example, the direction of arrival or direction of departure), leading to an enhanced ranging accuracy. Further applications cover the detection of breast cancer [26] and mine localization [71], as well as the detection of fires by active UWB radiation [261].

Even though a typical power increment (array gain) by multiple antennas is noticed, a general investigation on bandwidth dependence substantiated by quantitative results is still missing. In general, it is evident that a boost of bandwidth is accompanied by a diminished small-scale fading. Hence, a threshold region will exist, but this is not yet quantified. Exceeding this region makes UWB-SIMO less promising, because only the array gain persists.

Overall, the research on UWB-MIMO is still in its infant stage. Further studies, especially on its implementation, are necessary to bring this technology into the market.

1.5 Scope of This Book

We conclude this chapter with a brief overview of the areas discussed in the remainder of this book.

Chapter 2: *UWB-MIMO Channel Measurement and Models*. Since the monopulses used in UWB radios are very narrow, the received pulses from different paths with a time difference on the order of nanoseconds can be resolved. Owing to this fact, a UWB channel model will be fundamentally different from that of narrowband communications. In this chapter, several commonly used UWB channel models are briefly introduced, which will form the basis of subsequent chapters. The channel sounding equipment developed in our institute and the ray-tracing simulation tool, which is used to simulate the impulse or frequency response of general communication channels, are also presented. The ray-tracing simulation tool is very helpful for investigating the channel model when experimental facilities are limited.

Chapter 3: *UWB Channel Capacity*. In this chapter we investigate how the channel capacity of UWB-MIMO depends on the numbers of transmit and receive antennas. The results will provide some guidelines for how to use multiple antennas to increase the data rates of UWB communication systems. Three cases are investigated: MISO, SIMO and MIMO. We show in each case that the data rate will increase with the number of antennas in a different way; and in some extreme case for MISO, increasing the number of transmit antennas will be detrimental to the data rate. This is peculiar to UWB systems.

Chapter 4: *UWB-MIMO Space–Time Coding*. An essential objective of using MIMO is to increase the data rate by its inherent multiplexing gain and/or diversity gain. Different from the narrowband communication channel, the UWB-MIMO channel may exhibit diversities in more dimensions: in the time domain (multipaths) or frequency domain in addition to the spatial domain. A simple yet widely used STC scheme for narrowband wireless communications is the Alamouti code. In the literature, two kinds of STC schemes, which are similar to the Alamouti code, were proposed for IR-based UWB-MIMO systems. In this chapter we first briefly introduce these two coding schemes and investigate their performance. We show that different coding schemes work well in different SNR ranges. After that, we discuss a general design approach for the STC of

IR-based UWB systems with arbitrary numbers of transmit and receive antennas. This design approach is based on real orthogonal design . The concept of the companion of real orthogonal design is proposed for easing the decoding. Finally, a review of the spatio-frequency multiplexing problem and spatio-time–frequency coding is presented for MB UWB systems.

Chapter 5: *UWB Beamforming and Localization*. As mentioned above, UWB Beamformers have some special properties that are quite different from narrowband beamformers. In this chapter we first investigate how these properties appear in UWB beamformers. Three types of UWB beampattern are defined. The optimal beamformer is presented. Using a UWB beamformer to find the direction of arrival or to estimate the locations of sources is discussed. In principle, the UWB localization problem is similar to the sparse-path radar ranging problem, but the former has both peculiar advantages and great challenges due to very narrow UWB pulses. The main advantage is that its resolution is very high, since the received UWB pulses scattered from different objects can be resolved even if the objects are separated by several centimetres. The main challenge is that mature detection algorithms for the relevant pulse are not yet available, since the received signal consists of so many paths that it is extremely difficult to identify which path is relevant to the object we are concerned with. A UWB array may provide a promising approach to identifying the locations of the objects. By properly processing the two-dimensional signals, only one peak will appear. It is important to investigate the relationship between the peak and the location of the object. In the second part of this chapter, several approaches to the UWB localization problem are examined: beamforming, time of arrival (ToA), and mapping. The methods for dealing with NLOS and multipaths are reviewed and some new relevant ideas discussed.

Chapter 6: *Time-Reversal UWB Systems*. The TR technique has been applied extensively in acoustic and medical applications and underwater communications. Reports have demonstrated that, in the ultrasonic frequency regime, it is possible to provide error-free communications with five receivers simultaneously. Because of the peculiar property of UWB channel impulse responses, namely abundant multipaths, the TR idea can find wide applications in UWB radios. In this chapter we investigate several fundamental issues in TR-UWB-MIMO systems: why, instead of other kinds of filters, should the TR filter be used at the transmitter and what is the effect of imperfect channels on the system performance? To answer the first question, we analyse the performance of the system with relevant pre-filters at the transmitter when the original channel is of nonminimum phases or corrupted by some estimation errors. To address the second question, we examine how the bit error rate (BER) and received SNR of the TR system change when only a part of the original channel can be obtained and channel estimation errors are suffered. In this chapter we also show that, with an appropriate pre-equalizer, using the TR technique can perform multiuser communications via either MIMO, MISO, or SIMO, combined with the UWB radio. The corresponding pre-equalizer design is presented.

Chapter 7: *UWB Relay Systems*. Owing to the spectral mask applied to UWB transmission, the transmit power is limited. Thus, the coverage of regularized UWB communication systems is limited to a few metres. To increase the coverage, one possible way is to use multihop relaying. In this chapter we study the system performance of two-hop UWB relay systems in terms of BER, SNR outage probability and the amount of fading. These systems consist of the following: the source, relay and destination can be equipped with single/multiple antennas, the receivers at the relay and destination can perform coherent or noncoherent detection, and the CSI can be available at the transmitters of the source and relay or at the receivers of the relay and destination. Some guidelines on the design of UWB-MIMO relay systems are illustrated via the analytical and simulation results.

1.6 Notation

Throughout the book we use $\mathbf{I}$ to denote an identity matrix, whose dimension is indicated by its subscript if necessary; $P_A(x)$ and $p_A(x)$ respectively represent the cumulative distribution function (cdf) and probability density function (pdf) of a random variable A; $\mathbb{E}$ (or $\mathbb{E}_A$ if necessary) stands for the expectation of a random quantity with respect to the random variable A; and $\mathbb{E}(\cdot|\cdot)$ denotes the conditional expectation. For a matrix or vector, the use of superscript T, $*$ and $\dagger$ denote the transpose, the element-wise conjugate (without transpose) and the Hermitian (conjugate) transpose respectively. The $*$ and $\dagger$ notation also apply to a scalar. The function log is naturally based, if the base is not explicitly stated. We use `diag` to denote a diagonal matrix with the diagonal entries being specified by the corresponding arguments.

For other notation, we might use the same symbol to denote different things in different chapters or sections. In such a case we will explicitly explain what the symbol stands for.